Integrated theoretical and empirical studies for probing substrate-framework interactions in hierarchical catalysts

Stephanie Chapman, Alexander J. O'Malley, Ivana Miletto, Marina Carravetta, Paul Cox, Enrica Gianotti, Leonardo Marchese, Stewart F. Parker and Robert Raja

Published version information

This is the peer reviewed version of the following article:

Citation: S Chapman et al. "Integrated theoretical and empirical studies for probing substrate-framework interactions in hierarchical catalysts." Chemistry: A European Journal, vol. 25, no. 42 (2019): 9938-9974.

DOI: 10.1002/chem.201901188

Which has been published in final form at DOI above. This article may be used for non-commercial purposes in accordance with Wiley-VCH terms and conditions for self-archiving.

Please cite only the published version using the reference above. This is the citation assigned by the publisher at the time of issuing the AAM. Please check the publisher's website for any updates.

Integrated theoretical and empirical studies for probing substrate-framework interactions in hierarchical catalysts

Stephanie Chapman,[a] Alexander J. O'Malley,[b, c, d] Ivana Miletto,[e] Marina Carravetta,[a] Paul Cox,[f] Enrica Gianotti,[e] Leonardo Marchese,[e] Stewart F. Parker,[b, g] Robert Raja*[a]

Abstract: Soft-templating with siliceous surfactant is an established protocol for the synthesis of hierarchically-porous silicoaluminophosphates (HP SAPOs) with improved mass transport properties. Motivated by the enhanced performance of HP SAPOs in the Beckmann rearrangement of cyclohexanone oxime to the nylon-6 precursor, ε-caprolactam, we have undertaken an integrated theoretical and empirical study to investigate the catalytic potential of the siliceous mesopore network. Neutron scattering studies, in particular, have provided unique insight into the substrate-framework interactions in HP (Si)AlPOs, allowing reactive species to be studied independent of the catalyst matrix. The spectroscopic (INS, FTIR, MAS NMR) and computational analyses reveal that in the organosilane-templated SAPO, the interconnectivity of micro- and meso-pores permits a cooperativity between their respective silanol and Brønsted acid sites that facilitates the protonation of cyclohexanone oxime in a physical mixture, at ambient temperature.

[a] Miss S Chapman, Dr M Carravetta, Prof R Raja
Department of Chemistry, University of Southampton
University Road, Southampton, SO17 1BJ, U.K.
E-mail: R.Raja@soton.ac.uk
[b] Dr A J O'Malley, Dr S F Parker
UK Catalysis Hub, Research Complex at Harwell
STFC Rutherford Appleton Laboratory
Chilton, Didcot, OX11 0QX, U.K.
[c] Dr A J O'Malley
Centre for Sustainable Chemical Technologies (CSCT)
Department of Chemistry, University of Bath
Claverton Down, Bath, BA2 7AY, U.K.
[d] Dr A J O'Malley
Cardiff Catalysis Institute,School of Chemistry
Cardiff University, Main Building
Park Place, Cardiff, CF10 3AT, U.K
[e] Dr I Miletto, Prof E Gianotti
Department of Science and Technological Innovation
Università del Piemonte Orientale
Viale T. Michel 11, 15121 Alessandria, Italy.
[f] Dr P Cox
School of Pharmacy and Biomedical Sciences and Institute of Biomedical and Biomolecular Sciences
University of Portsmouth
Portsmouth, PO1 2DT, U.K.
[g] Dr S F Parker
ISIS Pulsed Neutron and Muon Facility
STFC Rutherford Appleton Laboratory
Chilton, Didcot, OX11 0QX, U.K.

Supporting information for this article is given at the end of the document.

Introduction

The acid-catalyzed Beckmann rearrangement of cyclohexanone oxime is a fundamental step in the production of ε-caprolactam; a valuable bulk chemical and the precursor to nylon-6. Whilst large-scale production of caprolactam has conventionally employed a homogeneous acid-catalyst, a need to reconcile high industrial demand with important sustainability targets has motivated the design of targeted, solid-acid catalysts.[1]

Considerable progress has been made in the development of heterogeneous catalysts for the Beckmann rearrangement, and zeotype catalysts, in particular, have made a significant impact in this field.[2] In fact, the use of solid-acid catalysts in the vapor-phase Beckmann rearrangement process has afforded substantial improvements in the sustainability of large-scale caprolactam production.[3] Furthermore, as spectroscopic analyses and computational techniques have evolved, it has been possible to explore in more detail the structure-activity relationships that allow zeolitic catalysts to operate effectively in the Beckmann rearrangement. These investigations, which have focused predominantly on the industrial, vapor-phase process, have yielded two catalytic mechanisms (Figure 1), depending on whether the transformation is facilitated by weakly-acidic silanol sites, or stronger, Brønsted centers (of the type Si(OH)Al).[4]

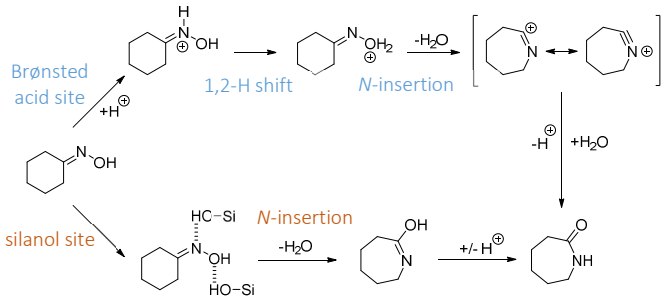

Figure 1. The two mechanistic pathways proposed for the Beckmann rearrangement of cyclohexanone oxime using solid-acid catalysts, invoking either Brønsted sites (blue) or silanols (orange).

Although calculations have shown that the Beckmann rearrangement occurs ~5 orders of magnitude faster at a Brønsted site than at a silanol nest,[4d] it is in fact the highly siliceous zeolites (having fewer Brønsted sites and a high density of silanol nests) that have proven most effective in the vapor-phase process, exhibiting higher yields and longer lifetimes.[5] The rationale is that at a Brønsted site, a high desorption energy for the bound lactam tends to suppress catalyst turnover and promote consecutive reaction, favoring by-products and coking.[4a, 6] Since the high temperatures of the vapor-phase reaction can overcome energetic constraints, weak acid sites are favored on account of their high selectivity towards caprolactam.

Fundamentally, to maximize productivity it is critical that catalysts are engineered with an acid strength that is tailored to the target process.[7] In the case of the Beckmann rearrangement, acid sites need to be sufficiently strong to bind the oxime substrate and yet still weak enough to release the lactam product once formed. However, such optimization requires an understanding of how acid site characteristics affect substrate-framework interactions and how this, in turn, modifies the catalytic outcome.

One technique that has proven informative in studying substrate-framework interactions is inelastic neutron scattering (INS).[8] Whilst optical vibrational spectroscopy is a typical method for characterizing surface-bound adsorbate, its sensitivity is often limited by the opacity of the zeolite and an inability to access informative, low-energy modes in the fingerprint region. However, in INS, spectra are dominated by modes involving significant proton motion. Since ^{1}H hydrogen has greater than tenfold larger incoherent scattering cross-section for neutrons than the elements comprising the zeolite, the framework is effectively transparent. As a result, neutron spectroscopy is ideally suited for studying key reactive moieties (such as the active sites and reactant species) in isolation of the catalyst matrix. Previously, we exploited the properties of neutron-based techniques in a quasi-elastic neutron scattering (QENS) experiment, contrasting the bulk diffusion of cyclohexanone oxime in microporous zeotypes for the Beckmann rearrangement.[9] More recently, we used INS to perform a detailed, vibrational characterization of the molecular species relevant to the Beckmann rearrangement.[10] Building on these fundamental studies, we now present INS as a tool to probe the atomic-level, substrate-framework interactions in the Beckmann rearrangement, with a view to ascertaining new mechanistic insights that could aid rational catalyst design. Moreover, we demonstrate how a diverse spectroscopic analysis can aid in understanding more complex catalytic systems;[11] namely hierarchically-porous silicoaluminophosphates (HP SAPOs).

Silicoaluminophosphates (SAPOs)[12] are a family of zeolitic frameworks that exist with a range of pore architectures and have proven potential as solid-acid catalysts.[13] The HP systems have been engineered to combine the desirable physicochemical characteristics of the parent SAPO with an auxiliary mesoporous network that enhances mass transport properties.[14] By adopting a soft-templating strategy and a siliceous, surfactant mesoporogen,[15] the resulting HP SAPOs are produced with pendant silanol sites in the mesopores, in addition to the Brønsted sites of the microporous framework.[16] Both silanol and Brønsted sites are acid centers with the potential to facilitate the Beckmann rearrangement, although the mode and degree to which they facilitate this process is unknown. Moreover, silanols are known to increase the polarity of internal channels,[17] which may encourage uptake of the oxime. Therefore, to establish whether the mesopores play an active role in catalyzing the transformation, or simply facilitate transport to Brønsted acid sites in the micropores, spectroscopic investigations have been undertaken.

To study the structure-property relationships that influence the activity of the HP and microporous (Si)AlPO catalysts, the interaction of HP SAPO-34 with cyclohexanone oxime was contrasted with its microporous analogue. Whilst both hierarchical and microporous SAPO-34 have proven activity in the vapor-phase Beckmann rearrangement,[16b] the low/ambient-temperature studies (undertaken for the purpose of mechanistic elucidation) accentuates the catalytic limitations of the narrow CHA windows. In fact, for microporous SAPO-34, the 3.8 Å micropore windows preclude access to cyclohexanone oxime and, as such, substrate-framework interactions are restricted to the external acid sites. Since the acid characteristics of microporous and hierarchical SAPO-34 frameworks are comparable,[16b] any difference in activity can be attributed to accessibility factors.

To ascertain whether the activity of HP SAPO-34 is due to the accessibility of the internal Brønsted sites, or whether the mesopore-based silanols make a catalytic contribution, the interactions of these sites also needs to be deconvoluted. As such, the interaction of hierarchical AlPO-5 with cyclohexanone oxime was studied, since this material possesses pendant silanols from surfactant soft-templating but lacks the Brønsted acid sites from isomorphous substitution of Si. Additionally, the AFI-type framework (7.3 Å pore diameter) of AlPO-5 does not present the same micropore size-constraints that otherwise inhibit the interaction of cyclohexanone oxime and CHA-type materials, allowing differences in catalyst activity to be attributed to the reactivity of the silanols. Using a combination of advanced characterization techniques (INS, probe-based FT-IR and solid-state NMR) with complementary computational studies, it has been possible to gain insight into the role of pore architecture and acid-site interactions in the Beckmann rearrangement (Figure 2).

Results and Discussion

The hierarchical catalysts were prepared using a soft-templating protocol,[15a, 16b, 18] the efficacy of which lies in the constitution of the siliceous surfactant mesoporogen.[15b] In an aqueous synthesis gel, the amphiphilic organosilane (dimethyloctadecyl[(3-(trimethoxysilyl)propyl] ammonium chloride, 'DMOD') spontaneously coalesces to form supramolecular micelles. The trimethoxysilyl components form covalent bonds between each other and the framework precursors, preventing expulsion of the micelles from the crystallizing microporous phase. On calcination, the organic component of the surfactant is eliminated and a hierarchically-porous (HP) structure is formed, with siliceous species incorporated into the walls of the mesopores.[19] As a result, the templating strategy has implications not only for the pore architecture but also the acid characteristics of the hierarchical frameworks.

	SAPO-34 (CHA)	HP SAPO-34 (CHA)	HP AlPO-5 (AFI)
Micropore diameter / Å	3.8	3.8	7.3
Mesopore diameter / Å	-	~ 30	~ 30
Nature of the active sites	Brønsted sites	Brønsted sites, silanols	silanols

Figure 2. The pore size diameters of the microporous and hierarchical catalysts studied herein, with a graphical representation of their framework structure and active sites. Key: orange = aluminium, white = oxygen, blue = phosphorous, purple = silicon.

Using the aforementioned synthetic procedure, crystalline, phase-pure HP AlPO-5 and HP SAPO-34 catalysts were prepared, their powder X-ray diffraction (XRD) spectra being consistent with AFI and CHA phases, respectively (Figure S1 and Table S1). Low-angle XRD showed a broad peak at 2θ ≈ 3.5 ° for HP SAPO-34 and at 2θ ≈ 1.5 ° for HP AlPO-5, which is indicative of some ordered mesoporosity, whereas SAPO-34 was featureless in the same region. Nitrogen adsorption studies (Figure S2 and Table S2) confirmed that the textural characteristics of HP AlPO-5, HP SAPO-34 and SAPO-34 catalysts were aligned with their expected values, and both hierarchical systems produced a Type IV isotherm (indicative of mesoporosity), whereas SAPO-34 yielded a Type I isotherm (characteristic of a microporous material). In addition, BJH analyses evidenced mesopores of diameter ~ 3 nm in both HP AlPO-5 and HP SAPO-34.

Inelastic neutron scattering experiments

To probe the interactions that drive the transformation of cyclohexanone oxime in the HP (Si)AlPOs, inelastic neutron scattering (INS) experiments were undertaken. In these studies, deuterated cyclohexanone-d10 oxime (CDO, $C_6D_{10}NOH$) substrate was used to remove the dominant vibrational modes of the cyclohexane ring. Since the incoherent scattering cross-section of H (80.27 barns) is much larger than D (2.04 barns), the oxime functional group of CDO could be targeted spectroscopically.

For reference purposes, the INS spectrum of cyclohexanone oxime was acquired (Figure 3a).[10] Crystallographic studies indicate that cyclohexanone oxime crystallizes in the $P\bar{3}$ space group, with asymmetric units that comprise of a hydrogen-bonded trimer (Figure 3b), where individual oxime molecules can both accept and donate hydrogen bonds.[20] As there is minimal interaction between the oxime trimers, the system was modelled as a single asymmetric unit, and the INS spectrum assigned by correlating experimental modes with computed vibrations, as reported in the literature.[10] Notably, heating the pure oxime in excess of its melting point (359 K) did not modify the appearance of its INS vibrational spectrum, indicating that intermolecular hydrogen bonding interactions within the oxime trimer were not irreversibly modified by thermal treatment, and that the crystal structure of the substrate was retained.

Figure 3. The INS vibrational spectrum of cyclohexanone oxime before (black) and after heating to 363 K (red) **(a)**. Key vibrational modes are identified as the in-plane N-O-H bend **(1)** and the out-of-plane N-O-H bend **(2)**. Also depicted is

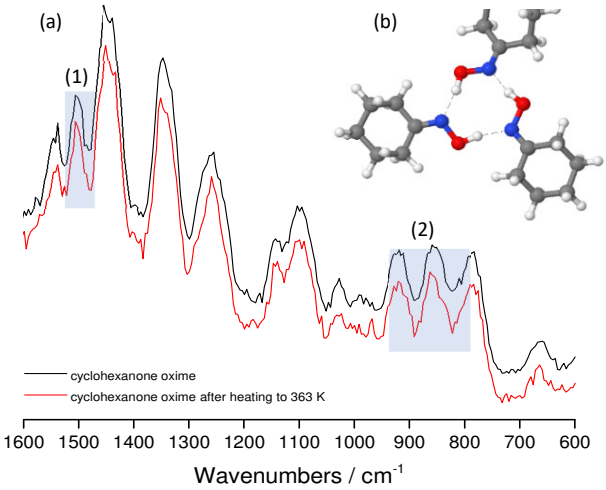

the hydrogen-bonding interaction between the NOH functionalities in a trimeric unit of crystalline cyclohexanone oxime **(b)**.

The INS spectra of the catalyst frameworks are presented in Figure 4. Where the main components of the HP AlPO-5 framework (Al, P, O) have a low scattering cross-section for neutrons, the INS spectrum of the empty framework is largely featureless. The exceptions are those framework modes that are made detectable by their association with hydrogen (a strong neutron scatterer). Therefore, the peak at 1125 cm^{-1} is assigned to the O-H bending mode of the pendant silanol sites in the mesopores, with possible contribution from P-OH or Al-OH defect sites. The corresponding O-H stretching mode is visible as a low intensity peak in the characteristic 3000-4000 cm^{-1} range.

Figure 4. INS spectra of SAPO-34 (top, green), HP SAPO-34 (middle, blue) and HP AlPO-5 (bottom, red), with the combination band of the stretching and out-of-plane bending mode of bridging OH group (1), O-H stretching (2), and O-H bending (3) modes highlighted.

The INS spectrum of SAPO-34 reveals more, intense O-H vibrational modes than HP AlPO-5, due to a greater quantity and

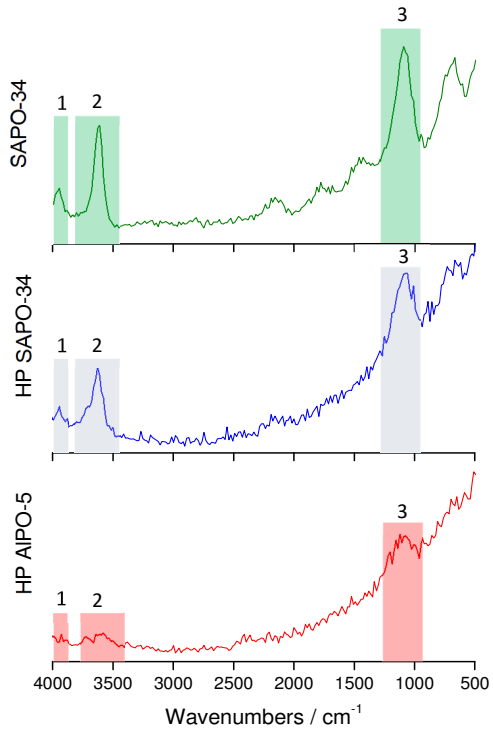

variety of acid sites from Type II and Type III substitution of Si. The band at 3625 cm^{-1} has been observed by diffuse-reflectance infrared analysis of SAPO-34,[21] and is assigned as the fundamental stretching vibration of Si(OH)Al groups. The corresponding bending mode is observed at 1100 cm^{-1},[22] and a combination band of the stretching and out-of-plane bending modes of the OH groups is detected at 3900-4000 cm^{-1}.[23] The vibrational INS spectrum of HP SAPO-34 is largely comparable to that of SAPO-34, with a few distinctions. Firstly, the O-H stretching band of the bulk Brønsted sites (3650 cm^{-1}) possesses a high-energy shoulder, which reveals its superposition with the broad, low-intensity stretching mode of the pendant silanols (identified in HP AlPO-5). Moreover, the HP SAPO-34 hydroxyl bands are, in general, broader than those in the microporous framework. This is likely due to structural disorder on introducing the mesoporous network.

Physical mixtures of CDO with each framework were analyzed by INS (Figure 5). For microporous SAPO-34/CDO (Figure 5a), the INS spectrum appeared as a superposition of the spectra of the component framework and oxime, which indicated that there was no significant interaction between catalyst and substrate. As well as retention of SAPO-34 framework bands, both the out-of-plane (OOP) and in-plane (IP) N-O-H bending modes (at 825 and 1600 cm^{-1}, respectively), and associated O-H stretching modes (2750-3250 cm^{-1}) of the oxime are identifiable. These observations confirm the inaccessibility of the internal active sites of SAPO-34 to cyclohexanone oxime, at low temperature. The pore-size restrictions of SAPO-34 are less problematic under the conditions of the vapor-phase Beckmann rearrangement, since rapid diffusion allows high turnover at the active sites on the catalyst surface and pore-mouths.[6b]

Contrastingly, for HP AlPO-5/CDO (Figure 5c), key vibrational modes of the substrate are altered. Firstly, the NO-H stretching region is modified. Peak intensity in the range 2750-3250 cm^{-1} is lost, and the remaining NO-H stretching bands are shifted ($\Delta\nu \approx$ +50 cm^{-1}) relative to the pure substrate. These observations are consistent with a loss of oxime-oxime hydrogen bonding, which results in a stronger and shorter isolated NO-H bond. Given the tendency of the oxime to retain its crystalline structure after heating, the disruption of the trimer in a physical mixture is significant. Disassembly of the trimer could be driven by (multiple) interactions with accessible silanols and this, in turn, may facilitate a subsequent acid-catalyzed transformation. In addition, the discrete OOP and IP N-O-H bending modes of cyclohexanone oxime (at 825 and ~1600 cm^{-1}, respectively) are lost, and instead a broad peak spanning 500-1500 cm^{-1} is observed. This may be a convolution of the discrete bending modes, with molecular motion constrained by hydrogen bonding to silanol sites of varying energy. A discussion of modifications in the framework modes of HP AlPO-5 is limited by the low intensity of these bands, although the SiO-H stretching mode appears to be absent in the HP AlPO-5/CDO mixture.

Despite the different constitution of their frameworks, the vibrational spectrum of HP SAPO-34/CDO (Figure 5b) bears close resemblance to that of HP AlPO-5/CDO, reinforcing the hypothesis that the mesopore-based silanols (common to both HP catalysts) are involved in ambient-temperature interactions with CDO. As in HP AlPO-5, there is evidence for the loss of oxime NO-H stretching modes and a blue-shift of the residual N-O-H band on exposure to HP SAPO-34. Again, this suggests that the silanols in the mesopores of soft-templated HP catalyst interact favorably with cyclohexanone oxime, and disrupt the stable hydrogen bonding between oxime molecules in the solid state. It is feasible that this interaction precedes protonation of the oxime at a Brønsted site, and allows the HP catalyst to facilitate the Beckmann rearrangement once energetic requirements are met. In HP SAPO-34, a loss of intensity at 3630 cm^{-1} (the region associated with framework Brønsted acid sites) is also notable, as this suggests that some internal active sites are accessible to the substrate *via* the mesopores.

FT-IR experiments

Further insight into the interaction between soft-templated catalysts and cyclohexanone oxime was achieved through probe-based infrared (FT-IR) spectroscopy. Complementary to INS, FT-IR is sensitive to non-hydrogenous functional group vibrations, allowing characteristic modes (such as the C=N bond of the oxime, and the C=O functionality in ε-caprolactam) to be identified.

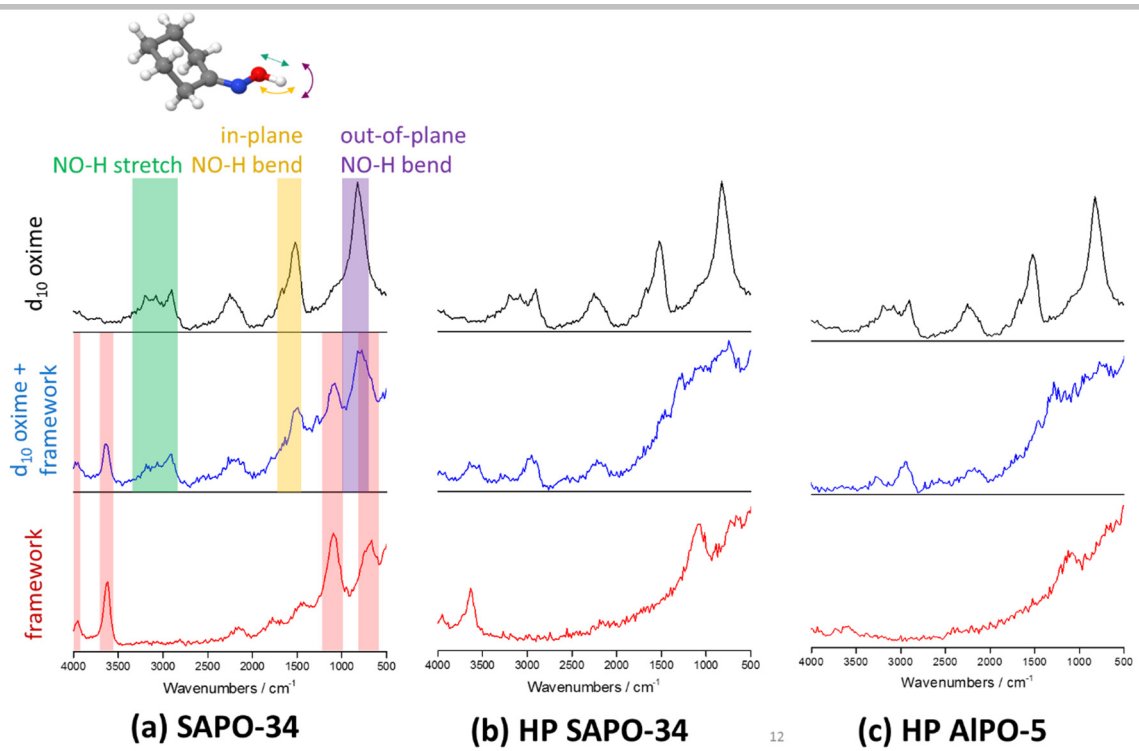

Figure 5. INS spectrum of cyclohexanone-d10 oxime (top, black line), empty framework (bottom, red line) and a physical mixture of the substrate and framework (middle, blue line) shown for SAPO-34 **(a)**, HP SAPO-34 **(b)**, and HP AlPO-5 **(c)**. Key framework and substrate bands are highlighted.

Firstly, the SAPO-34, HP SAPO-34 and HP AlPO-5 catalysts were outgassed at 300°C to remove adsorbed water and allow framework O-H stretching modes to be characterized (Table 1 and Figure S3). Microporous SAPO-34 exhibits two characteristic O-H stretching bands (at 3630 and 3600 cm^{-1}) that are attributed to Al(OH)Si Brønsted sites in the O(4) and O(2) framework configurations, respectively.[24] These Brønsted sites are also present, but less defined, in HP SAPO-34 where the mesoporous network introduces structural disorder. In HP SAPO-34 and HP AlPO-5, pendant silanols can be identified by the SiO-H stretching mode at ~ 3745 cm^{-1}. In addition, a weak PO-H stretching band at ~ 3678 cm^{-1} (from defect sites) is evident in all catalysts.[25]

Table 1. Catalyst O-H stretching modes identified by FT-IR spectroscopy.

O-H stretching mode	Band position / cm^{-1}	Framework		
		SAPO-34	HP SAPO-34	HP AlPO-5
Si-OH	3745	×	✓	✓
P-OH	3678	✓	✓	✓
Si(OH)Al Brønsted sites	3630, 3600	✓	✓	×

The FT-IR spectra of the three catalysts following exposure to cyclohexanone oxime are reported in Figure 6. In the high frequency region, the intensity of the O-H stretching modes is universally diminished by exposure to the oxime. However, for microporous SAPO-34, it is apparent that only a small fraction of the Brønsted sites (i.e. those accessible at the surface) interact with the oxime. In contrast, adsorption of oxime entirely eliminates the Brønsted O-H bands in HP SAPO-34. The implication is that the mesopores and micropores are interconnected, allowing cyclohexanone oxime to be protonated by the internal Brønsted sites, at ambient temperatures. Note that the asymmetric and symmetric CH_2 stretching (2935 and 2860 cm^{-1}) and $\delta(CH_2)$ modes (1450 cm^{-1}) characterize the oxime.

Figure 6. The FT-IR spectra of HP AlPO-5 (curve a, red), HP SAPO-34 (curve b, blue) and SAPO-34 (curve c, green) before (dotted lines) and after (solid lines) exposure to cyclohexanone oxime, at room temperature.

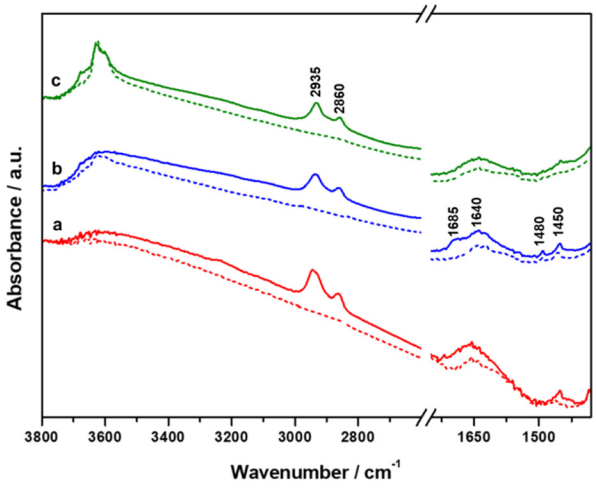

In the low frequency region, a broad signal between 1700 - 1600 cm^{-1} is attributed to the C=N stretching mode of cyclohexanone oxime, perturbed by the interactions between the N atom of the oxime and OH groups in the catalyst.[4c] Notably, for HP SAPO-34, a shoulder at ~1685 cm^{-1} is assigned to the $C=N^+$ stretching mode of protonated oxime.[26] Since the shoulder is absent in HP AlPO-5, the indication is that stronger Brønsted acid sites are

needed for protonation to proceed at room temperature. In HP SAPO-34, the substrate-activating effect of the mesopore silanols (identified by INS) and the improved accessibility of the internal Brønsted sites facilitates oxime protonation. The presence of the δOH band of cyclohexanone oxime (1480 cm^{-1}) is also consistent with *N*-protonation being preferred over *O*-protonation. These observations are consistent with earlier mechanistic studies that have identified the formation of *N*-protonated oxime prior to the rate-determining step.[4d]

MAS NMR experiments

In order to probe the low-temperature, silanol-substrate interactions revealed by INS and FT-IR, magic-angle spinning nuclear magnetic resonance (MAS NMR) studies were undertaken. Considering the ^{1}H NMR data for the calcined catalysts (Figure 7), the structure of the spectrum produced by SAPO-34 is consistent with that in the literature.[21] In general, peak intensity in the region of 1.2 - 2.3 ppm is attributed to the hydroxyl groups of framework defect sites and terminal silanols, whilst resonances between 3.6 - 4.4 ppm, are assigned to bridging OH groups (Si(OH)Al).[25b, 27]

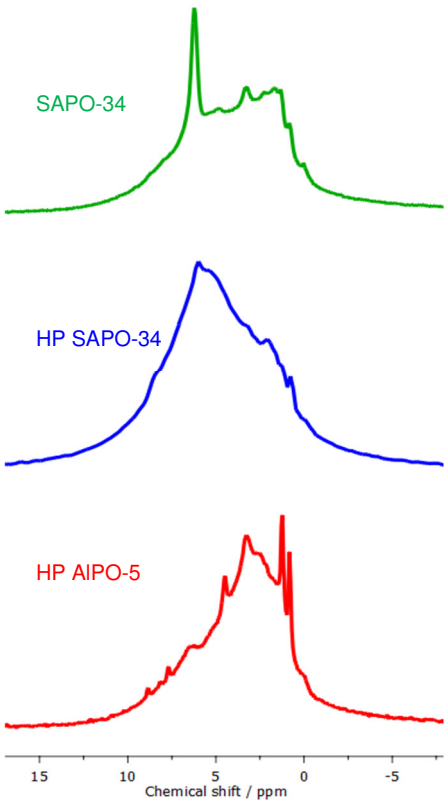

Figure 7. ^{1}H MAS NMR spectrum of HP AlPO-5 (bottom, red), HP SAPO-34 (middle, blue) and SAPO-34 (top, green) acquired at 600 MHz under a nitrogen atmosphere at ambient temperature. Spinning frequency 30 kHz.

Compared to SAPO-34 and HP SAPO-34, the ^{1}H MAS NMR spectrum of HP AlPO-5 lacks a relatively intense peak at 6.2 ppm, which is thus attributed to the Brønsted acid sites in the CHA-type frameworks. This is also consistent with discussions of O-H proton acidity in the literature, since proton deshielding (and hence acid strength) correlates with positive chemical shift.[28] HP AlPO-5 presents two sharp bands between 0 - 2 ppm, which are attributed to the weaker defect P-OH and Al-OH groups.[29] These can be resolved in HP AlPO-5, as they are not masked by the presence of the more abundant Brønsted site resonances. The broad signal observed in the HP systems covering a chemical shift range of 0 - 5 ppm may be associated with the pendant silanols; the amorphous nature of the mesopores yielding a relatively ill-defined proton environment. Finally, the proton spectrum of HP SAPO-34 appears as a convolution of the spectra obtained for SAPO-34 and HP AlPO-5, reflecting the presence of both the bulk Brønsted sites and the pendant silanol groups in the mesopores. The proton spectrum of the substrate, cyclohexanone oxime, reveals two intense peaks: a broad, intense resonance centred at 1.8 ppm due to the ring methylene protons, and a peak at 11.1 ppm from the oxime NOH functionality (Figure S4).[27b] More specifically, the downfield resonance is attributed to oxime in the hydrogen-bonded trimeric units of the crystalline phase; intermolecular interactions may be responsible for the downfield shift in the O-H resonance relative to isolated oxime molecules in solution (9 - 10 ppm).[28]

Focusing on the downfield region, in a physical mixture of SAPO-34 and cyclohexanone oxime, two resonances are identified by ^{1}H MAS NMR (Figure 8a). As well as the NOH resonance of crystalline oxime (11.1 ppm), an additional resonance is detected at 10.1 ppm. The latter is assigned to the NOH proton of a small fraction of isolated oxime molecules, hydrogen-bonded to external Brønsted acid sites on SAPO-34. The simultaneous downfield shift of the framework Brønsted acid proton resonance from 6.2 ppm to 6.4 ppm is also indicative of hydrogen bonding interactions with the NOH functionality. The peak developed at 5.7 ppm is assigned to *N*-hydrogen bonding between the oxime and an acid site of the catalyst, with the Brønsted sites (at 6.2 ppm) shielded on accepting electron density from the nitrogen lone pair. This interaction would be consistent with the proposed mechanism of the Beckmann rearrangement, which is initiated by *N*-protonation of the oxime by the framework. There is negligible change in the ^{1}H NMR spectrum on heating the SAPO-34/oxime sample, and overall retention of the peak at 11.1 ppm indicates that some oxime remains in the crystalline state. Thus, INS, FT-IR and ^{1}H MAS NMR studies of the SAPO-34/oxime mixture indicate that substrate-framework interactions are limited for the microporous CHA system.

When combined with the hierarchically-porous catalysts, distinct modifications are observed in the ^{1}H NMR spectrum of cyclohexanone oxime. Firstly, considering the downfield region of the HP AlPO-5/oxime mixture (Figure 8b), there is a single peak at 10.0 ppm, which indicates complete disruption of the solid oxime structure through (*O*-hydrogen bonding) interaction with the mesopore-based silanols. In HP SAPO-34 (Figure 8c), at room temperature there is evidence of both crystalline (11.0 ppm) *O*-hydrogen-bonded oxime (9.9 ppm) but on heating to 50 °C, only the latter is observed. Thus, it appears that at room temperature, the transfer of oxime into the mesopores is incomplete because (unlike the AFI structure of AlPO-5) the and

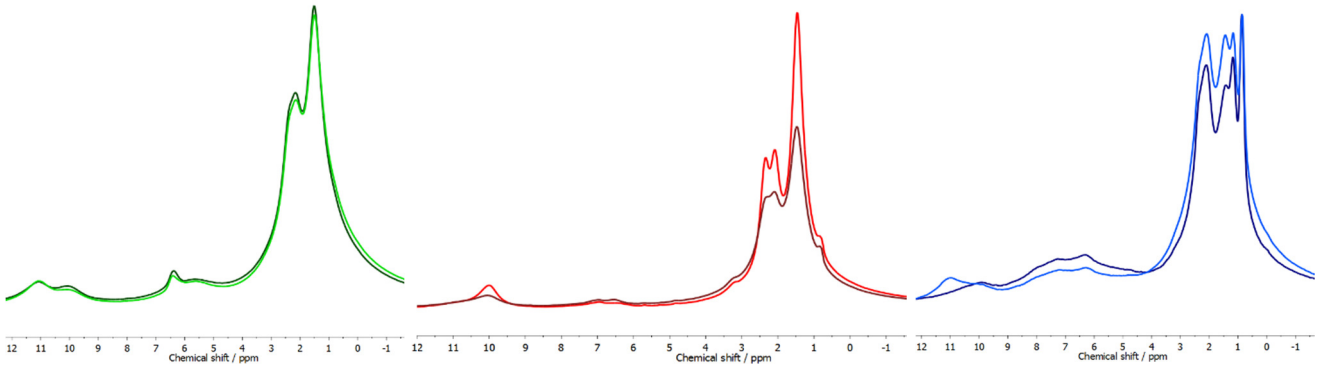

Figure 8. The ^{1}H MAS NMR spectra of SAPO-34 **(a)**, HP AlPO-5 **(b)**, and HP SAPO-34 **(c)** in a physical mixture with cyclohexanone oxime before and after heating to 50 °C for 2 hours. Spectra acquired at 600 MHz and a spinning frequency of 30 kHz.

CHA structure offers no possibility of ingress *via* the micropores. Nonetheless, ^{1}H NMR spectra indicate that, in a solid-state mixture, the oxime substrate will interact with the framework silanols, made accessible by their location in the mesopores.

Both HP catalysts exhibit two peaks in the 5-8 ppm region on combination with cyclohexanone oxime. These peaks are attributed to N-H species, which are known to produce ^{1}H resonances in a similar region (~ 6.5 ppm).[27b] N-H resonances are also consistent with the Beckmann rearrangement mechanism, and align with our previous assignment of the SAPO-34/oxime ^{1}H NMR spectrum. The range of resonances observed in this region indicates an array of N-H bond strengths, from weak hydrogen bonding, through to complete *N*-protonation. Thus, in HP SAPO-34, it is possible that the two peaks are observed where the oxime can engage in both *N*-hydrogen bonding (6.3 ppm) with the weak silanol sites, and also undergo full *N*-protonation by the stronger Brønsted acid sites in the bulk (7.2 ppm) - as is the indication from FT-IR studies. The interactions at the oxime nitrogen atom may be facilitated by the same *O*-hydrogen bonding interactions that disrupt the structure of the solid oxime, and also maintain the isolated molecules in proximity of the framework.

Computational studies

To reinforce the spectroscopic assignments, computational modelling was used to assess the binding and protonation energies of cyclohexanone oxime at Brønsted and silanol acid sites. First, the energy of a hydrogen-bonded, trimeric oxime unit was compared to three isolated oxime molecules, and found to be 181 kJ mol^{-1} more stable. A single molecule of cyclohexanone oxime was then docked on the surface of a silanol-terminated mesopore, emulating the soft-templated structures of the HP catalysts. As indicated in Figure 9, of the two principal hydrogen-bonding configurations available at the silanol surface, the *N*-acceptor interaction (Figure 9a) of the oxime was found to be most stable (-184 kJ mol^{-1}), which is consistent with the rearrangement mechanism. Additionally, the *O*-acceptor interaction (Figure 9b) was also significantly stabilizing (-165 kJ mol^{-1}), which is consistent with the previous MAS NMR assignments. Importantly, the interaction of three isolated oxime molecules *via* *N*-acceptor interaction with the siliceous surface (3 x -184 kJ mol^{-1} = -552 kJ mol^{-1}) is significantly larger than the stabilization energy for the oxime trimer (-181 kJ mol^{-1}), providing an energetic driving force for the separation of the trimer within the mesopores.

Figure 9. Cyclohexanone oxime hydrogen-bonded to the surface of an MCM-41 cluster *via* (a) the oxime nitrogen atom (N-H distance = 1.531 Å) and (b) the oxime oxygen atom (O-H distance = 1.563 Å).

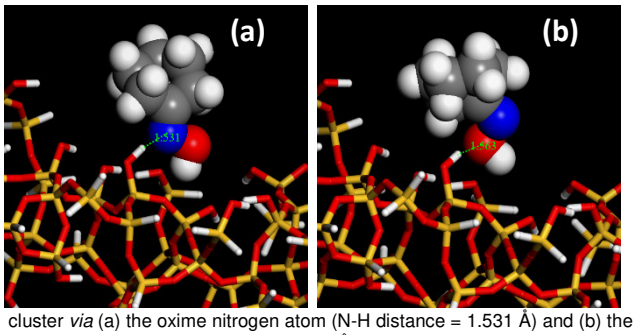

The binding energy of cyclohexanone oxime at a Brønsted site on the surface of a SAPO-34 crystallite was also calculated with optimized geometries (Figure 10). Given the low loading of Si in the SAPO catalysts, these bridging acid sites were treated as spatially-isolated. Although the binding energies *via* *N*-acceptor interaction (-242 kJ mol^{-1}) and *O*-acceptor interaction (-238.9 kJ mol^{-1}) were similar, again the *N*-acceptor configuration was (marginally) more favorable. Notably, the calculations reveal that an oxime molecule is more strongly bound by a Brønsted site than a silanol site. Also, the deprotonation energies at the Brønsted sites for SAPO-34 (+1242 kJ mol^{-1}) were lower than those for the silanol acid sites in a mesopore (+1371 kJ mol^{-1}), which correlates with the protonation of oxime observed spectroscopically. We therefore propose a mechanism of adsorption and interaction with the hierarchical catalysts, based on a consideration of both the spectroscopic and computational findings. First, the solid oxime trimer is separated into isolated molecules by hydrogen bonding with silanol sites that are accessed within mesopores. This interaction activates the oxime molecules, predominantly through *N*-hydrogen bonding interactions (with some contribution from *O*-hydrogen bonding).

In the case that Brønsted acid sites are also available (as in HP SAPO-34), there is an energetic driving force for the transfer of the oxime from the weak silanol sites in the mesopores, to the stronger Brønsted centers in the proximal micropores, and from here, protonation (Figure 1) can proceed more readily.

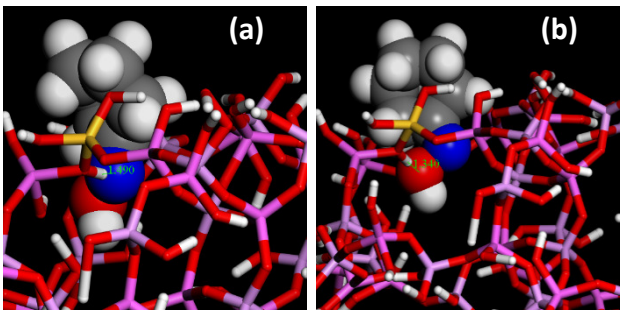

Figure 10. Cyclohexanone oxime hydrogen-bonded to the surface of a SAPO-34 cluster *via* (a) the oxime nitrogen atom (N-H distance = 1.490 Å) and (b) the oxime oxygen atom (O-H distance = 1.340 Å).

Conclusions

To gain further insight into how the nature of the active sites and how their interactions can influence the heterogeneously-catalyzed Beckmann rearrangement, a combined spectroscopic-computational study of hierarchical (Si)AlPO catalysts was undertaken.

Spectroscopic analyses found limited interaction between cyclohexanone oxime and microporous SAPO-34 at ambient temperatures, with spectral features attributed to the framework Brønsted acid sites largely retained on exposure to the oxime. These observations reflect the inaccessibility of the internal Brønsted sites *via* the CHA pores under the conditions required for these fundamental studies. In contrast, when cyclohexanone oxime was combined with a HP catalyst, significant substrate-framework interactions were observed. Where INS studies indicated that weakly-acidic silanol sites within the mesopores disrupt the stable, hydrogen-bonded trimer of the solid oxime, DFT calculations found this to be an energetically favorable process. Notably, HP SAPO-34 is the only system where there is (MAS NMR and FT-IR) evidence for the formation of the *N*-protonated oxime at ambient temperature. Since cyclohexanone oxime is not protonated by HP AlPO-5 under the same conditions, protonation by the weakly-acidic silanols can be excluded. Equally, there is no evidence of oxime protonation by the external Brønsted acid sites of SAPO-34, despite having similar acid characteristics to its hierarchical analogue.[16b] Therefore, in a physical mixture, neither Brønsted sites, nor silanols alone, effect protonation of cyclohexanone oxime.

We thus propose that the enhanced catalytic performance of HP SAPO-34 can be attributed to the proximity of silanol and Brønsted acid sites, facilitated by interconnectivity of the mesopores and micropores. Based on computational and spectroscopic analyses, the indication is that the uptake of solid oxime occurs *via* the mesopores, where hydrogen bonding interactions with the local silanol sites leads to disintegration of the trimeric oxime structure. The isolation of the oxime molecules makes them available for activating interactions, predominantly through *N*-hydrogen bonding (and some *O*-hydrogen bonding) to the silanols. Where a proximal Brønsted acid site is made accessible through the interconnectivity of the micro- and mesoporous structures (as in HP SAPO-34), there is an energetic driving force for the oxime to bind to the stronger acid site, where a lower deprotonation energy facilitates *N*-protonation at ambient temperature. Then, with sufficient energetic input the transformation to ε-caprolactam can occur.

In summary, the organosilane mesoporogen generates siliceous mesopores in HP (Si)AlPO catalyst that modifies both the catalytic and mass transport characteristics of the microporous framework. The secondary mesoporosity in HP (Si)AlPO catalyst was found to improve the uptake of oxime into the microporous framework, and the silanols elicit catalytic activity in the HP (Si)AlPO framework. Crucially, where accessible silanols can work in synergy with Brønsted sites (as in HP (Si)AlPO), the Beckmann rearrangement proceeds via a hybrid mechanism (Figure 1), where the formation of a hydrogen bonded complex at the silanols, facilitates the protonation of oxime at a stronger Brønsted site. Ultimately, these spectroscopic and computational insights provide a mechanistic rationale that can be used to support the design of new, targeted acid-catalysts for the Beckmann rearrangement.

Experimental Section

Catalyst synthesis
Microporous and HP SAPO-34 catalysts were prepared as previously reported.[16b]

HP AlPO-5: Aluminium isopropoxide (54.5 g, Sigma Aldrich) was ground in a pestle and mortar and added to a stirred mixture of phosphoric acid (85 wt. % in H_2O, 18.2 mL, Sigma Aldrich) and deionized water (80 mL). After 1.5 hours stirring, dimethyloctadecyl[(3-(trimethoxysilyl)propyl] ammonium chloride (72 wt. % in H_2O, 9.6 mL, Sigma Aldrich), triethylamine (29.8 mL), and deionized water (160 mL) were added to the gel, which was stirred for a further 1 hour. The gel was transferred to a Teflon-lined, stainless steel autoclave and crystallized at 200 °C for 24 hours. The solid was collected by vacuum filtration, washed with deionized water (1 L), and dried overnight in an oven at 80 °C. The white solid was calcined under air for 16 hours, at 550 °C.

Synthesis of cyclohexanone-d10 oxime: In an ice bath, a 1:1 molar ratio of cyclohexanone-d10 (98 %, Sigma Aldrich) and hydroxylamine (50 wt. % in H_2O, Sigma Aldrich) were reacted, under stirring. After 1 hour, the white solid was collected by vacuum filtration, washed with ice-cold, deionized water (200 mL), and dried under vacuum.

Characterization:
Powder X-ray diffraction patterns were acquired using a Bruker D2 diffractometer with Cu $K_{\alpha 1}$ radiation. Unit cell refinements were performed using the CelRef software (LMGP-Suite for the interpretation of X-ray Experiments, by Jean Laugier and Bernard Bochu, ENSP/Laboratoire des Matériaux et du Génie Physique). Low-angle X-ray diffraction patterns were obtained using a Rigaku SmartLab diffractometer with Cu rotating anode source. Nitrogen adsorption measurements were performed at 77K using the Micromeritics Gemini 2375 surface area analyser. Prior to measurement, samples were degassed under vacuum at 120 °C for 12 hours.

Inelastic neutron scattering measurements were carried out at the ISIS Pulsed Neutron and Muon Source (Oxfordshire, UK).[30] Calcined catalysts were dried in an Inconel can at 350 °C, under a flow of He gas (0.25 SLPM) and then transferred to an Ar glove box. Catalyst-cyclohexanone-d10 oxime samples were prepared as a 10:1 mixture by grinding in a pestle and mortar. The empty frameworks, catalyst-oxime mixtures, and reference compounds (cyclohexanone-d10 oxime, ε-caprolactam-d10 (QMX Laboratories Ltd.)) were each transferred to a separate aluminium foil sachet, and sealed in a flat aluminium can. In addition, the sealed catalyst-oxime samples were heated in a fan-assisted oven at 50 °C for 2 hours to encourage thermal mixing. Analyses were performed using the high-resolution INS spectrometers MAPS[8b] and TOSCA.[31] Sample cans were placed in a top-loading closed cycle refrigerator cryostat and spectra collected at < 10 K to suppress the Debye-Waller factor. Spectra were assigned using Jmol software to visualize the vibrational modes calculated using density-functional perturbation-theory-based CASTEP calculations.

For solid-state NMR measurements, catalysts were packed in a 2.5 mm rotor and dried overnight in a fan-assisted oven at 100 °C. Catalyst-substrate samples were prepared in a N_2 glove box by grinding cyclohexanone oxime in a 1:10 ratio with dried catalyst. Spectra were acquired on a Bruker Avance-II spectrometer operating at 14.1 T, equipped with a Bruker 2.5 mm triple resonance MAS probe, and tuned to ^{1}H (resonance frequency 600 MHz). ^{1}H spectra were referenced against adamantane at 1.8 ppm.[32] Nitrogen boil-off gas was used for bearing and drive gases for magic-angle spinning (MAS).

FT-IR spectra of self-supporting pellets were used a Bruker Equinox 55 spectrometer equipped with a pyroelectric detector (DTGS type) of 4 cm^{-1} resolution. Calcined catalysts were ground in a pestle and mortar and pelletized to a density of 2-10 mg cm^{-2}. Self-supported pellets (~ 1 cm^2) were transferred to a specially-designed quartz cell with potassium bromide window. Calcined catalysts were pre-treated at 300 °C under vacuum and then cooled to ambient temperature to acquire a framework spectrum. Whilst under vacuum, the catalyst was then exposed to a vapor pressure of cyclohexanone oxime for 10 minutes and a FT-IR spectrum acquired. Finally, the oxime-dosed catalyst was heated to 130 °C for 30 minutes, cooled to ambient temperature and a FT-IR spectrum acquired. FT-IR spectra were normalized with respect to pellet density and, wherever stated, difference spectra show a subtraction of the pre-treated catalyst from that with adsorbed oxime.

Computational studies

Density functional theory (DFT) calculations were performed using the program DMol^3.[33] All calculations were performed using double numerical plus polarization (DNP) basis sets with geometry optimizations carried out by treating the exchange-correlation interaction with the generalized gradient approximation (GGA) using the Becke-Lee-Yang-Parr (BLYP) exchange-correlation functional.[34] Dispersion correction was applied using the method of Tkatchenko and Scheffler (TS).[35] Clusters of MCM-41 (447 atoms) and SAPO-34 (CHA) (260 atoms) were generated from previously published structures[36] and terminated with H atoms. Three convergence tolerances were set for the geometry optimizations, these were: energy change ≤ 2 x10^{-5} Ha, maximum force ≤ 0.004 Ha $Å^{-1}$, and maximum displacement ≤ 0.005 Å.

Acknowledgements

The resources and support provided by the UK Catalysis Hub *via* membership of the UK Catalysis Hub consortium and funded by the EPSRC (grants EP/K014706/1, EP/K014668/1, EP/K014854/1, EP/K014714/1 and EP/M013219/1) are gratefully acknowledged. The project leading to these results has also received funding from the European Union's Horizon 2020 Research and Innovation Programme, under grant agreement N. 720783 - MULTI2HYCAT. AJOM would like to acknowledge the Ramsay Memorial trust for provision of a Ramsay Fellowship, and Roger and Sue Whorrod for the funding of the Whorrod Fellowship. SC thanks AdvanSix Inc. for their support in funding her studentship. The STFC Rutherford Appleton Laboratory is thanked for the provision of neutron beamtime.

Keywords: Hierarchical architectures • solid-acid catalysts • Beckmann rearrangement • advanced characterization • neutron spectroscopy • probe-based FTIR • solid-state NMR • computational modelling

[1] A. B. Levy, R. Raja, M. E. Potter, US Pat., 9662643 B2, **2017**.

[2] S. Chapman, M. Potter, R. Raja, *Molecules* **2017**, *22*, 2127.

[3] a) I. Yoshitaka, I. Hiroshi, S. Yasumoto, K. Masaru, S. Hiroshi, *Bull. Chem. Soc. Jpn.* **2007**, *80*, 1280-1287; b) H. Sato, K. Hirose, N. Ishii, Y. Umada, US Pat., 4709024A, **1987**.

[4] a) V. R. Reddy Marthala, Y. Jiang, J. Huang, W. Wang, R. Gläser, M. Hunger, *J. Am. Chem. Soc.* **2006**, *128*, 14812-14813; b) V. R. Reddy Marthala, S. Rabl, J. Huang, S. A. S. Rezai, B. Thomas, M. Hunger, *J. Catal.* **2008**, *257*, 134-141; c) C. Flego, L. Dalloro, *Micropor. Mesopor. Mater.* **2003**, *60*, 263-271; d) T. Bucko, J. Hafner, L. Benco, *J. Phys. Chem. A* **2004**, *108*, 11388-11397; e) E. Gianotti, M. Manzoli, M. E. Potter, V. N. Shetti, D. Sun, J. Paterson, T. M. Mezza, A. Levy, R. Raja, *Chem. Sci.* **2014**, *5*, 1810-1819.

[5] a) H. Ichihashi, M. Kitamura, *Catal. Today* **2002**, *73*, 23-28; b) H. Ichihashi, M. Ishida, A. Shiga, M. Kitamura, T. Suzuki, K. Suenobu, K. Sugita, *Catal. Surv. Asia* **2003**, *7*, 261-270.

[6] a) J. Sirijaraensre, J. Limtrakul, *Phys. Chem. Chem. Phys.* **2009**, *11*, 578-585; b) T. Takahashi, M. N. A. Nasution, T. Kai, *Appl. Catal. A: Gen.* **2001**, *210*, 339-344.

[7] M. E. Potter, D. Sun, E. Gianotti, M. Manzoli, R. Raja, *Phys. Chem. Chem. Phys.* **2013**, *15*, 13288-13295.

[8] a) M. O. Jones, A. D. Taylor, S. F. Parker, *Appl. Petrochem. Res.* **2012**, *2*, 97-104; b) S. F. Parker, D. Lennon, P. W. Albers, *Appl. Spectrosc.* **2011**, *65*, 1325-1341; c) A. J. O'Malley, S. F. Parker, C. R. A. Catlow, *Chem. Commun.* **2017**, *53*, 12164-12176.

[9] M. E. Potter, A. J. O'Malley, S. Chapman, J. Kezina, S. H. Newland, I. P. Silverwood, S. Mukhopadhyay, M. Carravetta, T. M. Mezza, S. F. Parker, C. R. A. Catlow, R. Raja, *ACS Catal.* **2017**, *7*, 2926-2934.

[10] S. Chapman, A. J. O'Malley, S. F. Parker, R. Raja, *ChemPhysChem* **2018**, *19*, 3196-3203.

[11] G. Paul, C. Bisio, I. Braschi, M. Cossi, G. Gatti, E. Gianotti, L. Marchese, *Chem. Soc. Rev.* **2018**.

[12] B. M. Lok, C. A. Messina, R. L. Patton, R. T. Gajek, T. R. Cannan, E. M. Flanigen, *J. Am. Chem. Soc.* **1984**, *106*, 6092-6093.

[13] H. Pastore, S. Coluccia, L. Marchese, *Annu. Rev. Mater. Res.* **2005**, *35*, 351-395.

[14] a) M. Hartmann, *Angew. Chem. Int. Ed.* **2004**, *43*, 5880-5882; b) A. Erigoni, S. H. Newland, G. Paul, L. Marchese, R. Raja, E. Gianotti, *ChemCatChem* **2016**, *8*, 3161-3169.

[15] a) M. Choi, R. Srivastava, R. Ryoo, *Chem. Commun.* **2006**, 4380-4382; b) M. Choi, H. S. Cho, R. Srivastava, C. Venkatesan, D.-H. Choi, R. Ryoo, *Nat. Mater.* **2006**, *5*, 718.

[16] a) A. B. Levy, R. Raja, S. H. Newland, S. R. Keenan, S. R. Bare, US Patent 20160167030 A1, **2016**; b) S. H. Newland, W. Sinkler, T. Mezza, S. R. Bare, M. Carravetta, I. M. Haies, A. Levy, S. Keenan, R. Raja, *ACS Catal.* **2015**, *5*, 6587-6593.

[17] M. A. Camblor, A. Corma, H. García, V. Semmer-Herlédan, S. Valencia, *J. Catal.* **1998**, *177*, 267-272.

[18] Q. Sun, N. Wang, D. Xi, M. Yang, J. Yu, *Chem. Commun.* **2014**, *50*, 6502-6505.

[19] D.-H. Lee, M. Choi, B.-W. Yu, R. Ryoo, *Chem. Commun.* **2009**, 74-76.

[20] M. Lutz, A. L. Spek, R. Dabirian, C. A. van Walree, L. W. Jenneskens, *Acta Crystallogr. Sect. C: Cryst. Struct. Commun.* **2004**, *60*, 127-129.

[21] B. Zibrowius, E. Löffler, M. Hunger, *Zeolites* **1992**, *12*, 167-174.

[22] S. Coluccia, L. Marchese, G. Martra, *Micropor. Mesopor. Mater.* **1999**, *30*, 43-56.

[23] S. A. Zubkov, L. M. Kustov, V. B. Kazansky, I. Girnus, R. Fricke, *J. Chem. Soc., Faraday Transactions* **1991**, *87*, 897-900.

[24] a) L. Smith, A. K. Cheetham, L. Marchese, J. M. Thomas, P. A. Wright, J. Chen, E. Gianotti, *Catal. Lett.* **1996**, *41*, 13-16; b) I. Miletto, G. Paul, S. Chapman, G. Gatti, L. Marchese, R. Raja, E. Gianotti, *Chem. Eur. J.* **2017**, *23*, 9952-9961.

[25] a) G. V. A. Martins, G. Berlier, C. Bisio, S. Coluccia, H. O. Pastore, L. Marchese, *J. Phys. Chem. C* **2008**, *112*, 7193-7200; b) I. Miletto, C. Ivaldi, G. Paul, S. Chapman, L. Marchese, R. Raja, E. Gianotti, *ChemistryOpen* **2018**, *7*, 297-301.

[26] Y.-M. Chung, H.-K. Rhee, *J. Molec. Catal. A: Chem.* **2001**, *175*, 249-257.

[27] a) D. Freude, M. Hunger, H. Pfeifer, *Z. Phys. Chem.* **1987**, *152*, 171-182; b) V. R. Reddy Marthala, J. Frey, M. Hunger, *Catal. Lett.* **2010**, *135*, 91-97.

[28] D. Freude, *Adv. Colloid Interface Sci.* **1985**, *23*, 21-43.

[29] D. Freude, H. Ernst, M. Hunger, H. Pfeifer, E. Jahn, *Chem. Phys. Lett.* **1988**, *143*, 477-481.

[30] ISIS, http://www.isis.stfc.ac.uk/index.html, (accessed 01/10/2018).

[31] S. F. Parker, F. Fernandez-Alonso, A. J. Ramirez-Cuesta, J. Tomkinson, S. Rudic, R. S. Pinna, G. Gorini, J. F. Castañon, *J. Phys. Conf. Ser.* **2014**, *554*, 012003.

[32] H. Shigenobu, H. Kikuko, *Bull. Chem. Soc. Jpn.* **1991**, *64*, 685-687.

[33] B. Delley, *J. Chem. Phys.* **2000**, *113*, 7756-7764.

[34] A. D. Becke, *Phys. Rev. A* **1988**, *38*, 3098-3100.

[35] A. Tkatchenko, M. Scheffler, *Phys. Rev. Lett.* **2009**, *102*, 073005.

[36] a) P. Ugliengo, M. Sodupe, F. Musso, I. J. Bush, R. Orlando, R. Dovesi, *Adv. Mater.* **2008**, *20*, 4579-4583; b) L. S. Dent, J. V. Smith, *Nature* **1958**, *181*, 1794.

Supplementary Information for:

Integrated theoretical and empirical studies for probing substrate-framework interactions in hierarchical catalysts

Stephanie Chapman,[a] Alexander J. O'Malley,[b, c, d] Ivana Miletto,[e] Marina Carravetta,[a] Paul Cox,[f] Enrica Gianotti,[e] Leonardo Marchese,[e] Stewart F. Parker,[b, g] Robert Raja.[a]

a) Department of Chemistry, University of Southampton, University Road, Southampton SO17 1BJ, U.K.
b) UK Catalysis Hub, Research Complex at Harwell, Science and Technology Facilities Council, Rutherford Appleton Laboratory, Harwell Science and Innovation Campus, OXON, OX11 0QX, U.K.
c) Centre for Sustainable Chemical Technologies (CSCT), Department of Chemistry, University of Bath, Claverton Down, Bath, BA2 7AY, U.K.
d) Cardiff Catalysis Institute, School of Chemistry, Cardiff University, Main Building, Park Place, Cardiff CF10 3AT, U.K.
e) Department of Science and Technological Innovation, Università del Piemonte Orientale, Viale T. Michel 11, 15121 Alessandria, Italy.
f) School of Pharmacy and Biomedical Sciences and Institute of Biomedical and Biomolecular Sciences, University of Portsmouth, Portsmouth, PO1 2DT, U.K.
g) ISIS Pulsed Neutron and Muon Facility, Science and Technology Facilities Council, Rutherford Appleton Laboratory, Harwell Science and Innovation Campus, OXON, OX11 0QX, U.K.

Contents

Powder X-ray diffraction data

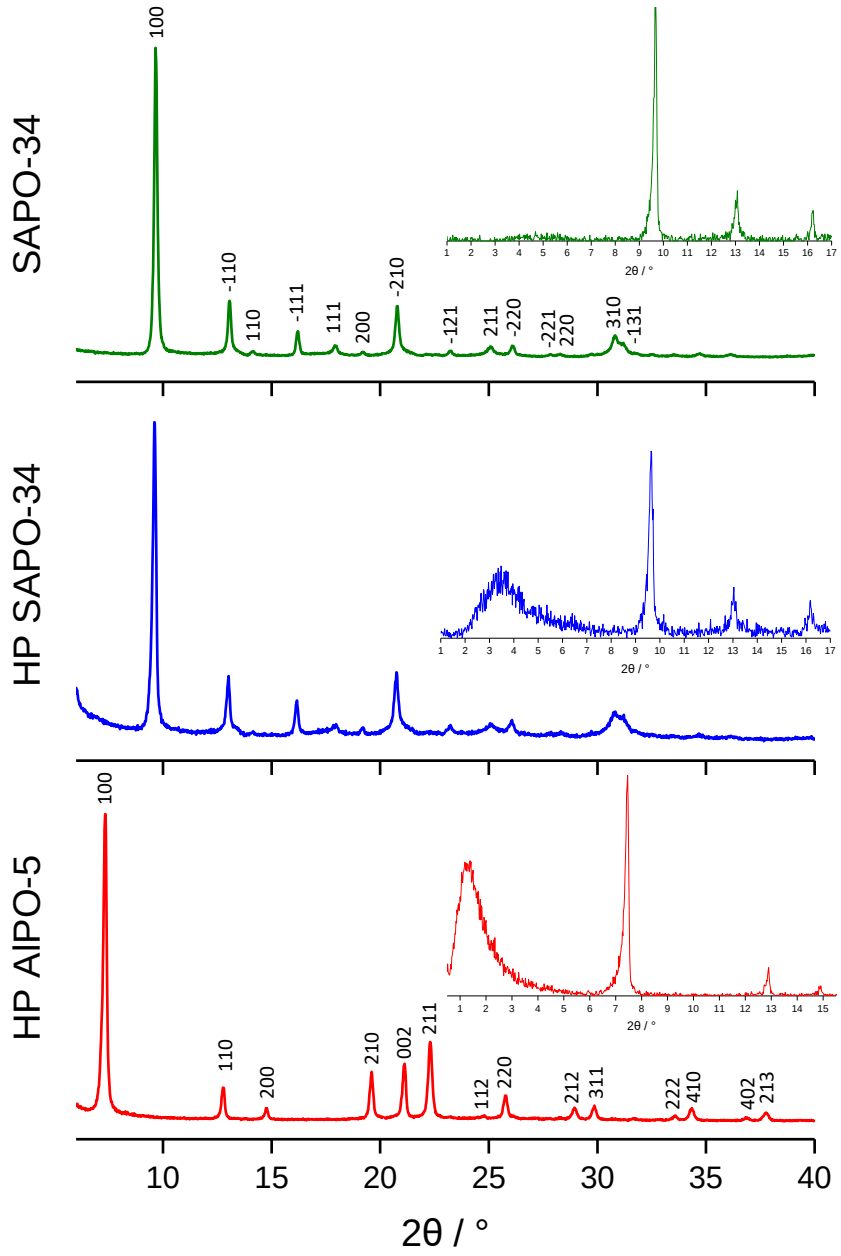

Figure S1: Indexed powder XRD pattern of SAPO-34 (top, green), HP SAPO-34 (middle, blue) and HP AlPO-5 (bottom, red), with their respective low-angle spectra inset.

Table S1: The experimental unit cell parameters for SAPO-34, HP SAPO-34 and HP AlPO-5 catalysts, with refinements performed using the CelRef software.[1]

Catalyst	Lattice Parameters				Space Group	Unit Cell Volume / Å^3
	***a* = *b* / Å**	***c* / Å**	**α = β / °**	**ϒ / °**		
SAPO-34	13.62	14.85	90	120	R-3m	2385
HP SAPO-34	13.64	14.85	90	120	R-3m	2393
HP AlPO-5	13.81	8.40	90	120	P6cc	1389

BET gas physisorption data

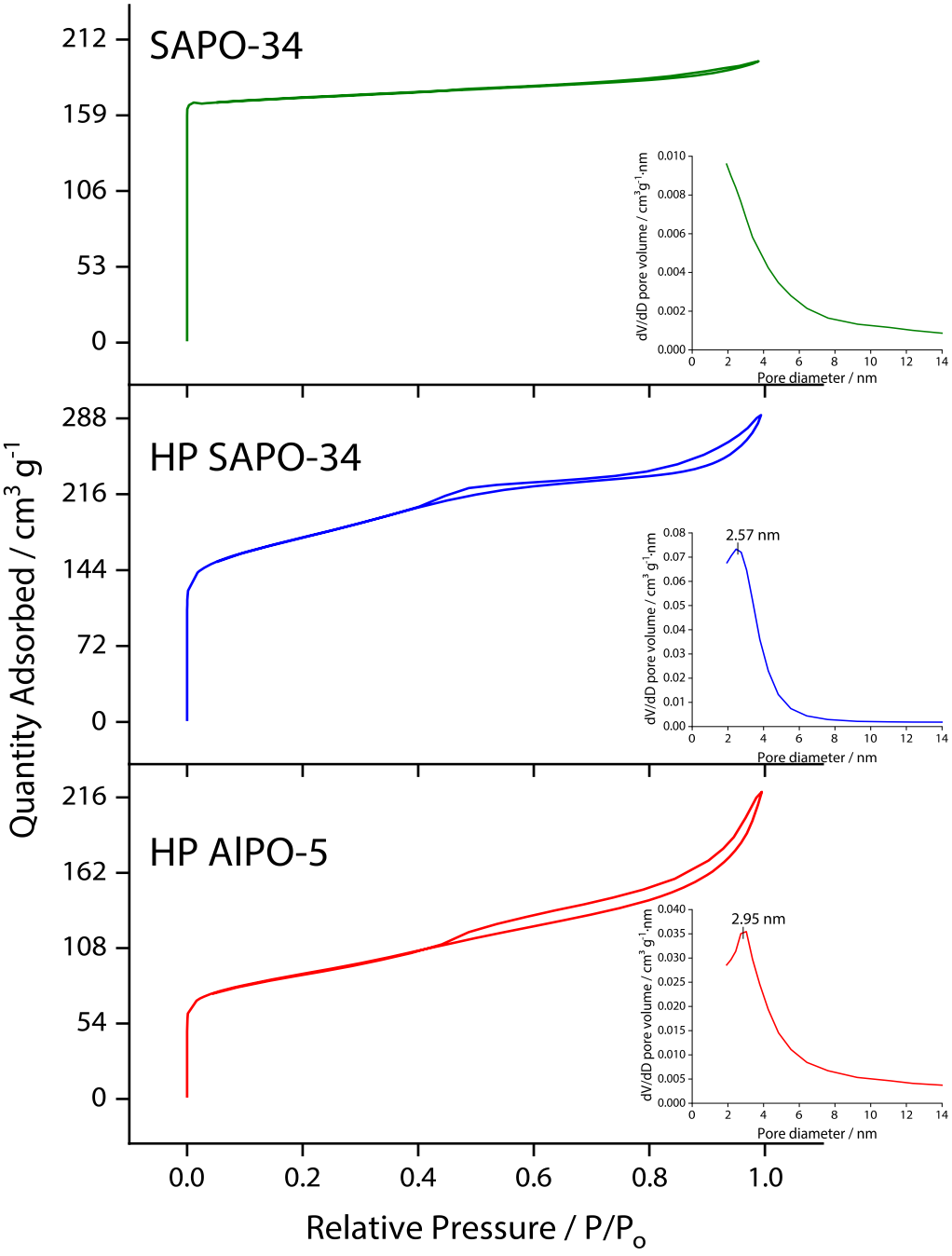

Figure S2: N_2 gas adsorption/desorption isotherm of SAPO-34 (top, green), HP SAPO-34 (middle, blue) and HP AlPO-5 (bottom, red) at 77K, with their respective BJH pore-size distribution inset.

Table S2: Textural properties of SAPO-34, HP SAPO-34 and HP AlPO-5 catalysts determined by N_2 adsorption/desorption studies.

Catalyst	S_{BET} / m^2 g^{-1}	V_{micro} / cm^3 g^{-1}	V_{meso} / cm^3 g^{-1}	External surface area / m^2 g^{-1}	Mesopore diameter / Å
SAPO-34	548	0.24	-	49	-
HP SAPO-34	589	0.13	0.14	319	26
HP AlPO-5	323	0.06	0.20	180	30

FT-IR spectra of catalysts

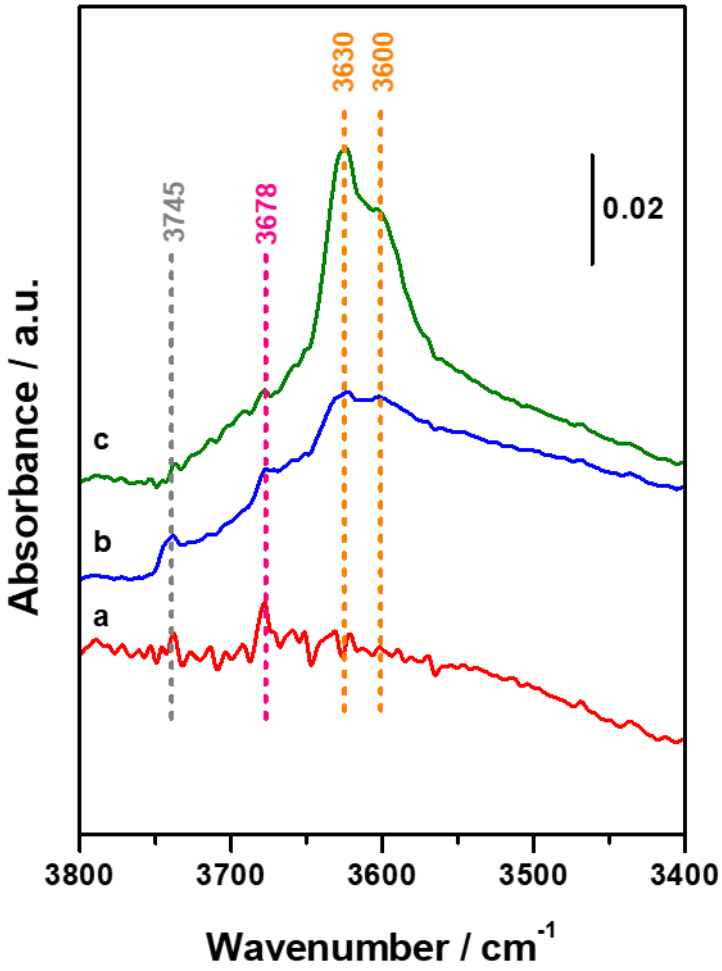

Figure S3: FTIR absorbance spectra in the O-H stretching region of HP AlPO-5 (curve a, red), HP SAPO-34 (curve b, blue) and SAPO-34 (curve c, green) with modes associated with Brønsted acid sites (orange), P-OH sites (pink) and Si-OH (grey) labelled.

Solid-state NMR spectrum of cyclohexanone oxime

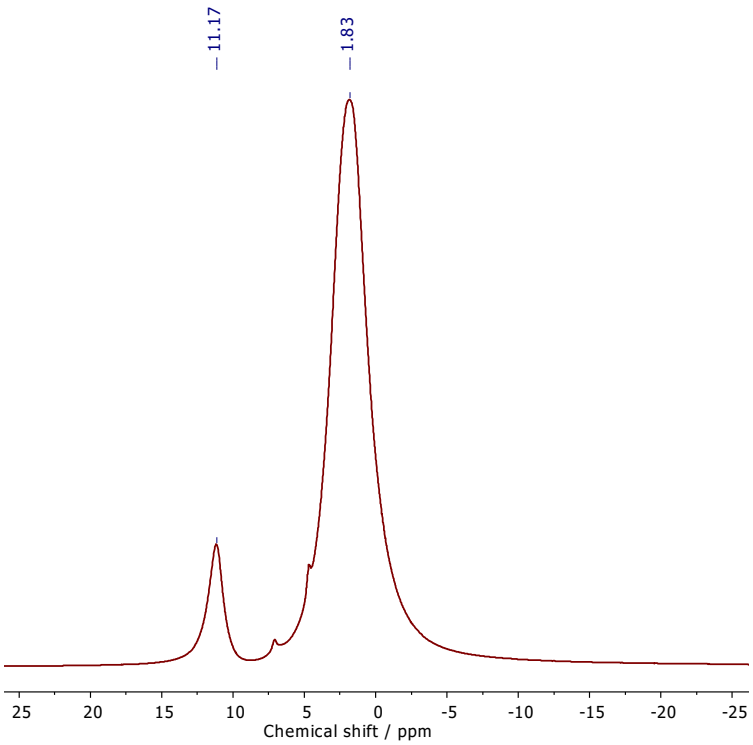

Figure S4: ^{1}H MAS NMR spectrum of cyclohexanone oxime acquired at 600 MHz and a spinning frequency of 27 kHz.

References:

1. Laugier, J.; Bochu, B. CelRef Version 3. http://www.ccp14.ac.uk/tutorial/lmgp/celref.htm.